Xylo-Oligosaccharide (XOS) Formation through Hydrothermolysis of Xylan Derived from Viscose Process

Alexandra Griebl,[1] *Thomas Lange,*[1] *Hedda Weber,*[1] *Walter Milacher,*[2] *Herbert Sixta**[2]

Summary: Xylo-oligosaccharides (XOS) have gained growing interest during the past decade owing to their beneficial influence on health. At the same time, a trend to a more effective utilization of biomass and biomass degradation products can be observed. As a consequence, also the steeping-lye of the viscose process is discussed as a potential source of new products based on xylans, xylooligosaccharides, xylose, and different xylose degradation products, thus being a driving force for the development of appropriate production processes. Therefore, xylan isolated from the steeping-lye was subjected to hydrothermal degradation for production of xylo-oligosaccharides (XOS). The experiments were carried out at 120, 150, and 180 °C, respectively. This hydrothermal treatment led to a soluble fraction, consisting of neutral and acidic XOS, and an insoluble residue predominantly made up of highly crystalline cellulose. A mass balance was established to calculate the activation energy for hydrothermal xylan degradation from weight loss kinetics. The degree of polymerization (DP) of the neutral product fraction could be influenced in a wide range by the reaction conditions applied. Acidic XOS were further characterized using mass spectrometry (MS). A 4-*O*-methylglucuronic acid residue α-(1,3)-linked to the xylose backbone was detected as a new structural element in alkaline degradation products derived from beech wood xylan.

Keywords: degradation; hydrothermolysis; polysaccharides; xylan; xylo-oligosaccharides (XOS)

Introduction

Hemicelluloses are the second most abundant natural polymer. Biomass and waste from biomass utilization are important sources for hemicelluloses. They also occur as intermediate products from sugar refinery or in a variety of industrial processes like for example viscose production[1,2]. The chemical and structural composition of hemicelluloses is highly dependent on their origin. Hemicellulose of beech wood, which is often used for viscose production, predominantly consists of xylan, with a xylose content of 19% based on wood. It has a β-D-(1,4)-linked xylopyranosyl backbone, which is substituted with α-D-(1,2)-4-*O*-methylglucuronic acid (4-*O*-MeGlcA) and with acetyl groups at *O*-2 and *O*-3[3]. The acetyl groups are linked almost equally to the 2- and 3-position of the xylose[4]. The ratio of 4-*O*-methylglcuronic acid to xylose in beech wood is approximately 10:1, additionally some arabinogalactan (2.9%) and glucomannan (1.5%) is found[3]. During acid sulfite pulping, arabinogalactan and glucomannan are completely hydrolysed[5]. The acetyl groups are cleaved too forming acetic acid[6]. Part of the xylan is solubilized and ends up in the cooking liquor, where it is degraded to low molecular weight xylans, xylose, xylonic acid,

[1] Competence Centre Wood Kplus, Werkstrasse 1, 4860 Lenzing, Austria
Fax: (+43) 7672 918 2930
E-mail: al.griebl@kplus-wood.at
[2] R&D Lenzing AG, Werkstrasse 1, 4860 Lenzing, Austria

© 2006 WILEY-VCH Verlag GmbH & Co. KGaA, Weinheim

and, to a low extent, to furfural and condensation products depending on the reaction conditions. Residual xylan in the pulp is further degraded by totally chlorine-free (TCF) bleaching. In the first step of viscose fiber production, the pulp is steeped with caustic (18 wt% NaOH) at slightly elevated temperatures removing part of the xylan. After pressing of the alkali-cellulose, the press-lye is led back into the steeping process. Thereby, the hemicellulose content is gradually increased until an equilibrium concentration is reached, when the hemicellulose leaving the system with the alkali-cellulose and with other bleeds equals the amount entering with the fresh pulp. It is commonly accepted, that dissolved hemicelluloses, exceeding a certain concentration, deteriorate both, processability and product quality. There are two ways of reducing the hemicellulose content in the system: either by using a highly purified dissolving pulp, which is a very expensive measure, or by dialyzing a certain press-lye fraction and removing the fraction rich in hemicelluloses from the system[7]. The hemicelluloses can be isolated from this dialyzed fraction rich in hemicelluloses by precipitation. This procedure yields a very pure and homogeneous product compared to hemicelluloses isolated from holocellulose by caustic extraction or from oat spelts[8] (Table 1). Hemicelluloses from viscose process therefore turn out to be a suitable source for the production of xylo-oligosaccharides (XOS) to be applied in the food sector. Such oligosaccharides have gained growing interest during the last decade owing to their impact on the health status of animals and humans[9]. Xylo-oligosaccharides show some additional physiological effects other oligosaccharides do not display[10,11].

Table 1.
Composition of hemicelluloses.

	beech holocellulose [8]	press-lye [7]	oat spelts [8]
xylose	76.2	95.6	75.8
arabinose	0	0	10.2
4-*O*-MeGlcA	14.2	-	2.3
other sugars	4.1	3.1	1.7
lignin	2.0	0	5.1

The degradation of xylan into XOS can be carried out by a variety of methods, including direct enzymatic conversion of susceptible raw materials, hemicellulose isolation followed by enzymatic hydrolysis[12,13], or autohydrolysis reaction[14,15]. In the latter case, the raw material is heated in an aqueous medium. The catalytic action of hydronium ions leads to the cleavage of the glycosidic bonds, resulting in the formation of XOS. Autohydrolysis carried out under mild reaction conditions allows selective depolymerization of the xylan backbone, leading to XOS as major reaction product. Depending on the severity of reaction conditions applied, autohydrolysis can result in the formation of sugars and sugar degradation products[16–19]. However, the autohydrolysis reaction is not specific, and impurities in the xylan are degraded as well as glucuronic acid side chains[20]. Depending on substrate composition, additional refining procedures may be necessary to improve the purity of the XOS concentrates, underlining again the importance of using pure substrates[21].

The objective of our investigation is to evaluate the hydrothermolysis process as a means to convert the hemicelluloses isolated from viscose process into XOS with controlled DP distribution. Understanding the chemical structure and reactions of XOS is a prerequisite for developing a new manufacturing process.

Experimental

Isolation and Characterization of Alkali Soluble Hemicelluloses from Press-lye

Hemicelluloses were isolated from press-lye by means of precipitation in diluted sulfuric acid at pH 2–3 (Figure 1). They consist mainly of xylose (95.6%), a small amount of glucose (3.1%) and of ash (0.23%). The isolated hemicelluloses are very pure and therefore will be referred to as xylan in this paper.

© 2006 WILEY-VCH Verlag GmbH & Co. KGaA, Weinheim

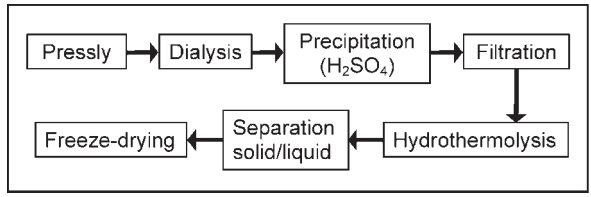

Figure 1.
Scheme of hemicellulose isolation and hydrothermolysis process.

Xylan shows a monomodal mass distribution, with a degree of polymerization (DP_n) calculated from Size-Exclusion Chromatography (SEC) being 56. Determination of carboxyl groups by methylene blue[22] resulted in a concentration of 266 μmol/g compared to 336 μmol/g of glucuronic acid determined according to Blumenkrantz[23]. Corresponding results (353 μmol/g) were obtained from Matrix-Assisted Laser Desorption/Ionisation Time-of-Flight Mass Spectrometry (MALDI-ToF-MS) measurements, at the same time, confirming their origin from 4-*O*-methylglucuronic acid side chains. Similar results were obtained before by Mais et al.[24] and Jacobs et al.[25].

Hydrothermolysis

Experiments were carried out in stainless steel reactors (volume: 40 mL, 3.5 cm outer diameter, 0.8 cm wall thickness), heated in oil baths. For hydrothermolysis experiments, 40 mL of xylan-water suspension (52,6 g/L solids concentration) were used. The reactors were heated in an oil bath having a temperature of 230 °C to minimize heating time. Shortly before the desired temperature inside the reactor was reached, the reactor was transferred into a second oil bath, being controlled at the target temperature of either 120, 150, or 180 °C, respectively. At 180 °C total reaction time was 45 minutes with samples being taken every 5 minutes. At lower temperatures reaction and sampling times had to be prolonged in order to achieve similar energy input. The reactions were quenched by immersing the reactors in an ice bath for 5 minutes. The liquid and solid contents were then transferred to centrifuge tubes and separated by centrifuging at 4000 rpm for 20 minutes. The liquid phase was decanted and passed through a 0.45 μm syringe filter. An aliquot of 7 mL was taken from each sample for measurement of pH value, furfural, XOS, and monomeric sugar composition. The remaining liquid phase as well as the solid residue were freeze-dried. After drying, the solid residue was weighed to establish a mass balance.

Monomeric Sugar Analysis

High-performance anion-exchange chromatography (HPAEC) with pulsed amperometric detection (PAD) was applied after total hydrolysis (TH) with H_2SO_4[7].

Furfural and Hydroxymethylfurfural (HMF) Analysis

High-performance anion-exchange chromatography (HPAEC) with UV-detection at 277 nm was applied before (hydrothermolysate) and/or after total hydrolysis (hydrothermolysate, solid residue). The column used was a Shandon Hypersil ODS 5μ, 4*250 mm with 14% acetonitrile as eluent at a flow rate of 0.9 mL/min. Measurements were carried out at 65 °C.

Neutral Xylo-Oligomers (XOS) and 4-*O*-Methylglucuronic Acid (4-*O*-MeGlcA) Analysis

High-performance anion-exchange chromatography (HPAEC) with pulsed amperometric detection (PAD) at a gold electrode was applied to the hydrothermolysate directly. The column was a Dionex CarboPac® PA 100 4*250 mm with a Dionex CarboPac® PA 100 Guard 4*50 mm precolumn operated at room temperature. The eluents used were 0.15 M NaOH (eluent A) and 0.15 M NaOH plus 0.5 M NaOAc (eluent B) at a flow rate of 0.5 mL/min. For

© 2006 WILEY-VCH Verlag GmbH & Co. KGaA, Weinheim

gradient program see Table 2. Quantification of XOS was effected using a calibration curve calculated from standards up to DP 6 and fucose as internal standard. Concentrations of XOS with a DP higher than 6 were calculated by extrapolation. Those extrapolated values could not be confirmed due to a lack of standards with higher DP.

Mass Spectrometry (MS)

Freeze-dried hydrothermolsate (12 mg) was dissolved in de-ionized water (1 mL). An aliquot (10 μL) of this sample was subjected to HPAEC-PAD, desalted using a Dionex CMD cation membrane desalter and collected in fractions of 0.5 mL. Every fraction was mixed with LiCl-solution (10 μL, 7 mmol/L) and injected into the mass spectrometer (Bruker Daltonics, Esquire 3000 plus) by direct infusion. Spectra were obtained in the positive mode. Peaks of particular interest were isolated and further fragmented (MS^2). The following parameters were used: flowrate: 4 μL/min; nebulizer: 15 psi; dry gas: 5 L/min; dry temperature: 250 °C; target mass: 500 (wide); compound stability: 100%; trap drive level: 100%; target: 50 000; scan: 50–2000 m/z; averages: 10; rolling: 2

Carboxyl Group Determination

Carboxyl groups were determined photometrically with methylene blue (MB) at 665 nm[22]. For glucuronic acid group determination *m*-hydroxy biphenyl (MHBP) and photometric detection at 520 nm were applied[23].

Size-Exclusion Chromatography (SEC)

The SEC system consisted of two PSS MCX, 1000 Å, 8 * 300 mm columns with refractive index detection at a flow rate of 1 mL/min of 0.5 M NaOH[7].

Table 2.
Gradient program for XOS-determination.

time [min]	eluent B [%]
0	5
30	30
31	100
37	100
38	5
43	5

Fourier Transform-Infra Red (FT-IR) Spectroscopy

FT-IR spectra were recorded on a Bruker Tensor 27 spectrometer with a liquid nitrogen cooled Mercury-Cadmium-Telluride (LN-MCT) detector at single reflection diamond Attenuated Total Reflexion (ATR) (''Golden Gate'') mode with a resolution of 2 cm^{-1}.

Solid-state Nuclear Magnetic Resonance (NMR) spectroscopy (^{13}C Cross Polarization/Magic Angle Spinning (CP/MAS) NMR)

The ^{13}C CP/MAS NMR measurements were performed on a 300 MHz Bruker DPX Avance-Spectrometer. A 7 mm probe head was used at a MAS-frequency of 4000 Hz and 100 scans were accumulated. The experiments were conducted at a cross polarization time of 2.2 ms and repeating times of 5 s.

Matrix-Assisted Laser Desorption/Ionisation Time-of-Flight Mass Spectrometry (MALDI-ToF-MS)

MALDI-ToF MS was carried out on an Ultraflex workstation (Bruker Daltronics GmbH, Germany) according to Kabel et al.[26].

Results and Discussion

Hydrothermolysis

The solid substrate xylan was degraded by hydrothermolysis into a soluble fraction, consisting of neutral and acidic XOS, and degradation products, and an insoluble fraction (Figure 2).

The extent of xylan hydrolysis depends on the chemical structure (side chains, position of side chains), temperature, time, acidity, and liquid-to-solid ratio[28]. Controlling the hydrothermolysis process necessitates an understanding of the kinetics of acid-catalyzed cleavage of xylan. The aim is to establish a relationship between

© 2006 WILEY-VCH Verlag GmbH & Co. KGaA, Weinheim

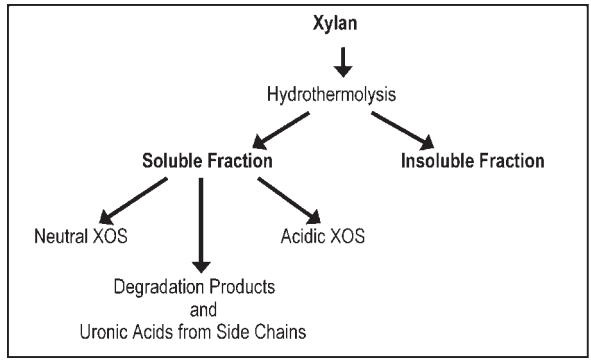

Figure 2.
Hydrothermolysis – overall-reaction.

the intensity of hydrothermolysis and the extent of xylan fragmentation.

Kinetic Modeling of the Hydrothermolysis of Xylan (Insoluble Fraction).

Assuming that xylan is completely accessible to water such that no diffusional restrictions affect the rate, and the local rate of xylan dissolution is proportional to the xylan concentration, the kinetics should follow first order in xylan. Our experimental results showed that xylan contains fractions of different reactivity as there is a distinct slowing of the rate at a certain extent of conversion. Therefore we concluded that xylan is composed of two fractions, each of them reacting according to a homogeneous first-order kinetics law, the rate of xylan hydrolysis can then be expressed according to the proposal of Veeraraghavan[27] and Conner[28]. The model is based on the presence of two types of xylan that hydrolyze via parallel first-order reactions:

$$-\frac{dX}{dt} = z_X \cdot k_{f,X} \cdot X_f + (1 - z_X) \cdot k_{s,X} \cdot X_s \quad (1)$$

X is the mass fraction of original xylan within the solid residue, consisting of X_f and X_s, the fractions of the fast- and slowly-reacting xylan, respectively. z_X is the fraction of the readily reacting xylan which has already been dissolved due to Hydrothermolysis reaction. $k_{f,X}$ and $k_{s,X}$ are the reaction rates of the fast- and slowly-reacting xylan, respectively, and t is the reaction time.

Since the fast reacting xylan constitutes more than 80% of the xylan, it may be sufficient to model only the fast reacting xylan using the following expression:

$$-\frac{dX_f}{dt} = k_{f,X} \cdot X_f \quad (2)$$

Hydrothermolysis was performed at a liquor-to-solid ratio of 19:1 in a series of five 40 ml autoclaves at three different temperature levels, 120 °C, 150 °C and 180 °C, respectively. Heating-up time was kept below 15 minutes and corrected for isothermal conditions using the following expression:

$$t_{T_o} = \int_{t_{T_t}}^{t_{T_0}} \mathrm{Exp}\left(\frac{E_A}{8,314} \cdot \left[\frac{1}{T_t} - \frac{1}{T_0}\right]\right) \cdot dt \quad (3)$$

where T_t is the temperature during heating-up, T_0 the target temperature, t_{T_0} the reaction time at target temperature, t_{T_t} the reaction time during heating up and E_A the activation energy. The use of corrected prehydrolysis time requires an iterative procedure. First, a value is assumed for activation energy, and the isothermal reaction time is calculated for each of the prehydrolysis experiments. A revised activation energy may then be calculated from an Arrhenius plot. The iterative procedure is repeated until the change in the activation energy becomes insignificant.

© 2006 WILEY-VCH Verlag GmbH & Co. KGaA, Weinheim

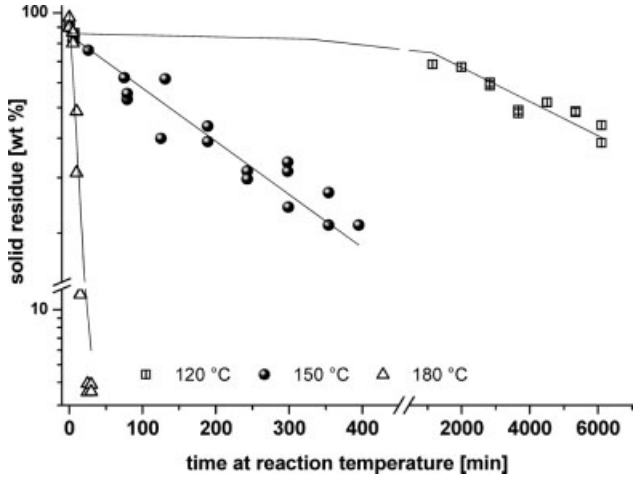

Figure 3.
Mass of xylan residue vs. reaction time (corrected for isothermal conditions) for hydrothermolysis of xylan isolated from press lye.

The results of weight-loss kinetics are shown in Figure 3

The kinetic parameters we calculated for the fast weight-loss reaction for water hydrothermolysis of xylan are compiled in Table 3.

To describe the intensity of hydrothermolysis, the H-factor principle[29] can be applied using an activation energy typical for the cleavage of glycosidic bonds of xylan (see Table 3). According to this principle the HT-factor (HTF) expresses the hydrolysis time and temperature as a single variable and is defined as

$$\mathrm{HTF} = \int_{t_0}^{t} k_{rel} \cdot dt \qquad (4)$$

in which k_{rel} is the relative rate of acid-catalyzed hydrolysis of glycosidic bonds, calculated from the relation of the rate constant of xylan hydrothermolysis at the temperature T ($k_{HT(T)}$) to the rate constant at 100 °C ($k_{100\,°C}$), which is assumed to be unity.

Inserting the determined activation energy for the fast reacting xylan, the relative rate is plotted against time, and the area under the curve represents the HTF.

$$\mathrm{HTF} = \int_{t_0}^{t} \frac{k_{HT(T)}}{k_{100°C}} \cdot dt = \int_{t_0}^{t} \mathrm{Exp} \cdot \left(54.69 - \frac{20407}{T}\right) \cdot dt \qquad (5)$$

This simple concept is illustrated by calculating the HTF-factor for a hydrothermolysis of one hour at constant temperatures. Hydrothermolysis for one hour at 150 °C and 160 °C corresponds to HTFs of 640 and 1950, respectively. The rate constants for hydrothermolysis more than triple for a 10 °C rise in temperature. It follows that to lower temperature from 160 °C to 150 °C, while keeping the hydrothermolysis intensity unchanged, the reaction time has to be expanded from 60 min to 183 min.

The applicability of the HTF-concept can be examined by plotting the remaining

Table 3.
Kinetic parameters for the weight-loss of xylan.

Temperature °C	$k_{f,x}$ min^{-1}		$E_{f,x}$ kJ/mol	
	average	stdev	average	stdev
120	1,25E-04	1,49E-05		
150	3,89E-03	3,39E-04		
180	9,47E-02	9,10E-03	169,7	0,4

© 2006 WILEY-VCH Verlag GmbH & Co. KGaA, Weinheim

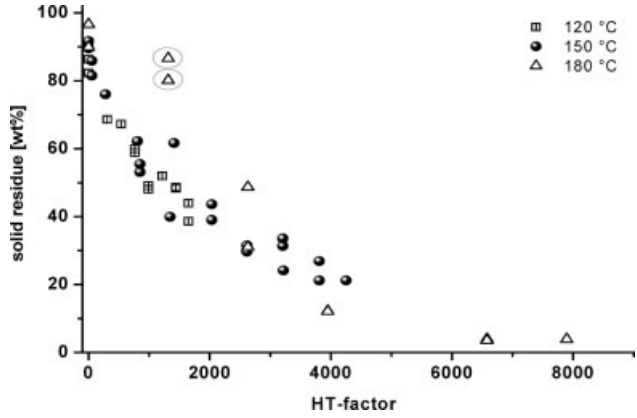

Figure 4.
Mass of xylan residue as a function of HT-factor for hydrothermolysis of xylan.

xylan content obtained by hydrothermolysis at three different temperatures against the HTF as shown in Figure 4:

Even though there is some scattering in the data – especially for the high temperature series – Figure 4 confirms that the HTF indeed bears a single relationship with the amount of the residual xylan at given temperatures.

Analytical Characterization of Insoluble Fraction.

SEC measurements suggested only small influence of reaction temperature on DP distribution of the residue, because comparable results were obtained for all experiments. Soon after the reaction was started a rather low DP was reached. Part of the alkali soluble initial substrate had been converted insoluble by hydrothermolysis and could not be included in the results. The amount of this fraction insoluble in both, sodium hydroxide solution and dimethylacetamide (DMA)/LiCl, seemed to increase with higher reaction temperatures.

FT-IR measurements could only confirm the presence of carbohydrates. With prolonged reaction time, bands became more distinct indicating a reduction in DP. At the same time, correspondence with the spectrum of viscose fibers was observed indicating an accumulation of glucan within the residue (Figure 5).

The lower stability of xylan towards autocatalytic/acidic degradation is known from literature to have both, physical and chemical reasons[30]. The acidic side chains of xylan inhibit the formation of tightly packed structures allowing at the same time easier access of water, thus facilitating hydrothermal, enzymatic, and acidic degradation compared to that of cellulose. Analysis of carbohydrate composition of the residue demonstrated glucan accumulation: after 35 minutes of reaction at 180 °C, the residue consisted of almost equal amounts of xylan and glucan. Results from reaction at 180 °C are presented in Table 4. to exemplify the trends observed at all temperatures.

The amount of total carbohydrates found in the residue decreased with increasing reaction time, especially at 180 °C, also suggesting a change in structure. This could be due to formation of degradation products (furfural) including further side reactions (e.g. condensation)[31–33]. The CP-MAS NMR spectrum of the residue shows two distinct peaks in the anomeric region at 109.0 and 107.8 ppm, respectively, that are characteristic for cellulose. The anomeric signal of xylan at 105.1 ppm has dissapeared, confirming the enrichment in glucan. At 86.1 and 84.1 ppm two signals for C-4 are present whilst the C-6 signal at 67.6 ppm is a singlet. These splitting patterns indicate highly

© 2006 WILEY-VCH Verlag GmbH & Co. KGaA, Weinheim

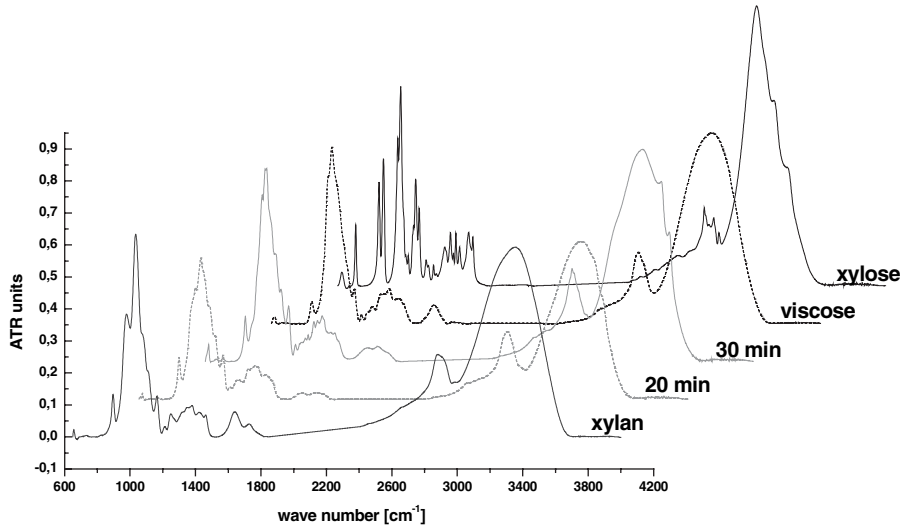

Figure 5.
IR spectra of xylan, xylose, viscose and residues after hydrothermolysis at 180 °C for 20, and 30 minutes, respectively.

cristalline cellulose II as described by VanderHart et al.[34]. Condensation products where Furfural is involved could not be detected (Figure 6).

Soluble Fraction

The soluble fraction consisted mainly of neutral and acidic XOS. Neutral XOS could be qualified as well as quantified using HPAEC-PAD while quantification of acidic XOS proofed impossible so far due to lack of standards. Accordingly, the total amount of XOS within the soluble fraction could only be determined indirectly using the mass balance.

Table 4.
Sugar composition of solid residue (in wt% of solid residue) after hydrothermolysis at 180 °C.

time [min]	xylose	glucose	total	yield
0	97.1	3.0	100.1	93.3
5	95.7	2.8	98.5	83.4
10	95.0	3.6	98.6	39.8
15	80.4	16.9	97.3	12.2
20	51.4	36.5	87.9	4.9
25	43.8	34.4	78.2	3.7
30	47.3	31.2	78.6	3.7
35	35.8	31.4	67.2	3.7
40	33.9	30.0	63.9	3.7
45	34.0	24.9	59.0	4.0

Neutral XOS in Soluble Fraction

As far as neutral XOS are concerned, reaction temperature had a rather large effect on XOS yield (Figure 7). During reaction at 180 °C, XOS yield reached a maximum after 15-25 minutes and decreased afterwards. At 150 °C, the same yield was reached as at 180 °C but after considerably longer reaction time. Within the reaction time investigated yield was constantly increasing so no maximum yield for hydrothermolysis at 150 °C could be determined. During reaction at 120 °C, yield did not even reach half the amount of the reaction at 150 or 180 °C even though reaction time was considerably prolonged.

Similar results were obtained for monomeric sugar composition of the total soluble fraction. The xylose yield was decreased from 44% of initial substrate at 180 °C to 17% at 120 °C while the amount of glucose slowly increased (Table 5).

DP distribution of the XOS was rather unaffected by reaction temperature but it strongly varied with reaction time. Again, reaction at 180 °C was chosen to depict results exemplarly in Figure 8. At the beginning of the reaction (up to 10 minutes), neutral XOS were obtained at a fairly even distribution over a DP range from 1 to 15

© 2006 WILEY-VCH Verlag GmbH & Co. KGaA, Weinheim

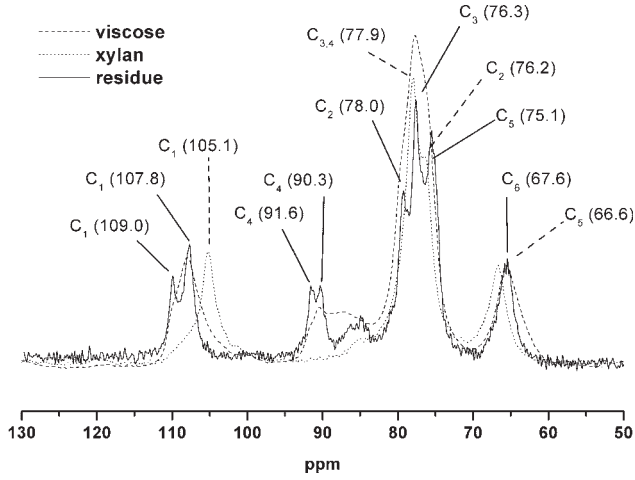

Figure 6.
^{13}C-CP/MAS NMR spectrum of initial xylan, viscose and solid residue after hydrothermolysis of 30 minutes at 180 °C.

but at a rather low yield. After 15 minutes the highest yield of total XOS as well as of XOS with a DP of two and higher could be obtained. Within this fraction yield was highest for xylobiose and decreased with increasing DP. Already twice as much xylose as xylobiose could be detected in this fraction. Further extension of reaction time led to an increase in xylose while yield of all other XOS including total yield decreased. For reaction times longer than 35 minutes yield of xylose decreased as well. Even though the effects described were comparable for all experiments, they were more distinct at higher reaction temperatures.

Presence of XOS with DP up to 18 could be confirmed by MALDI as well (Figure 9). The smalest detectable xylo-oligosaccharide was the sodium-adduct of xylotetraose at an m/z-ratio of 570. By adding multiples of 132, the molecular weight of anhydro xylose, to this m/z-ratio, the other neutral

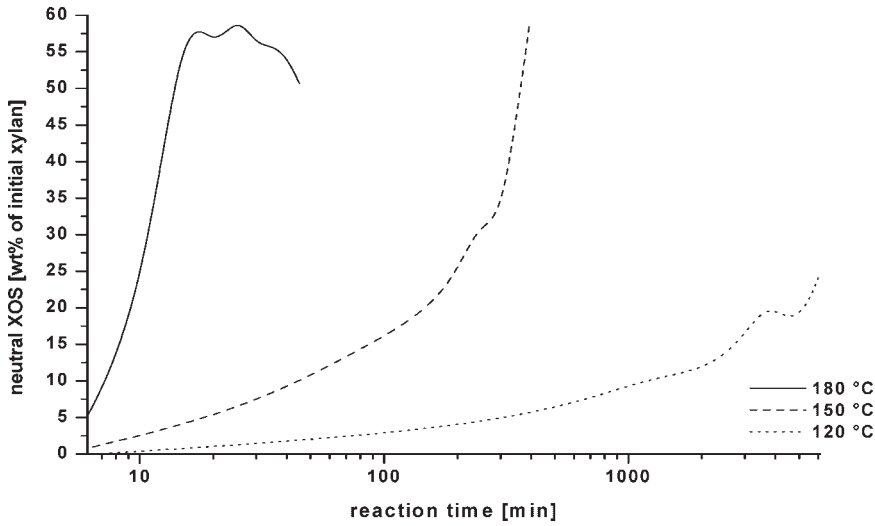

Figure 7.
Change in neutral XOS yield with reaction time and temperature.

© 2006 WILEY-VCH Verlag GmbH & Co. KGaA, Weinheim

Table 5.
Monomeric sugar composition of soluble fraction (in wt% of initial substrate).

180 °C				150 °C				120 °C			
time [min]	xylose	glucose	total	time [min]	xylose	glucose	total	time [min]	xylose	glucose	total
0	0.1	0.0	0.1	0	0.1	0.0	0.1	0	0.0	0.0	0.0
5	0.3	0.0	0.3	5	0.2	0.0	0.2	7	0.1	0.0	0.1
10	4.4	0.1	4.5	26	1.9	0.0	1.9	330	0.7	0.0	0.7
15	15.8	0.3	16.2	79	3.3	0.0	3.4	1145	2.8	0.0	2.8
20	18.8	0.5	19.3	131	6.4	0.1	6.5	1990	3.7	0.0	3.8
25	30.4	0.6	31.1	189	11.8	0.2	12.0	2830	6.3	0.1	6.3
30	36.4	0.8	37.2	243	19.7	0.3	20.1	3665	11.6	0.2	11.8
35	40.6	1.0	41.6	298	22.5	0.2	22.8	4505	10.6	0.1	10.7
40	43.5	1.2	44.7	354	29.1	0.4	29.5	5345	14.5	0.2	14.7
45	44.4	1.1	45.5	395	31.4	0.3	31.8	6105	16.7	0.2	16.9

XOS with higher DP, starting with xylopentaose, could be detected. Signal intensities of both, neutral and acidic XOS, decreased with increasing DP. Signals of neutral XOS showed a higher intensity than those of acidic XOS.

Acidic XOS in Soluble Fraction

To gain more information about the acidic XOS, the hydrothermolysate was subjected to MALDI measurements (Figure 9). Acidic XOS with a DP ranging from 3 to 17 could be detected, starting at an m/z-ratio of 627 for aldotetraouronic acid. Again, signals for acidic XOS with ascending DP could be identified by increasing the m/z-ratio by 132. All acidic XOS detected by MALDI carryied only one 4-*O*-MeGlcA side group each, at the same time confirming the absence of acetyl side groups. On the basis of MALDI measurements no conclusions could be drawn on the structure of the acidic XOS with regard to the exact position of the 4-*O*-MeGlcA side chain.

To further elucidate the structure of the acidic XOS, the hydrothermolysate was separated by HPAEC-PAD and analyzed by MS^2. Li-adducts ($Xyl_{2-16}MeGlcA\text{-}Li^+$)

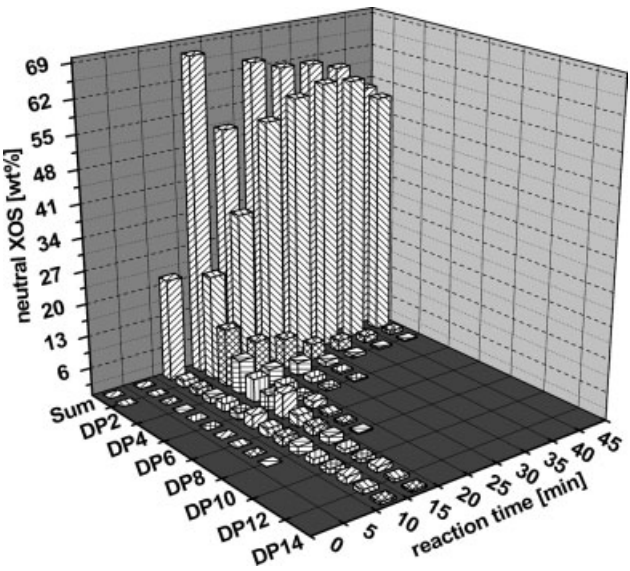

Figure 8.
Change in XOS distribution during reaction at 180 °C.

© 2006 WILEY-VCH Verlag GmbH & Co. KGaA, Weinheim

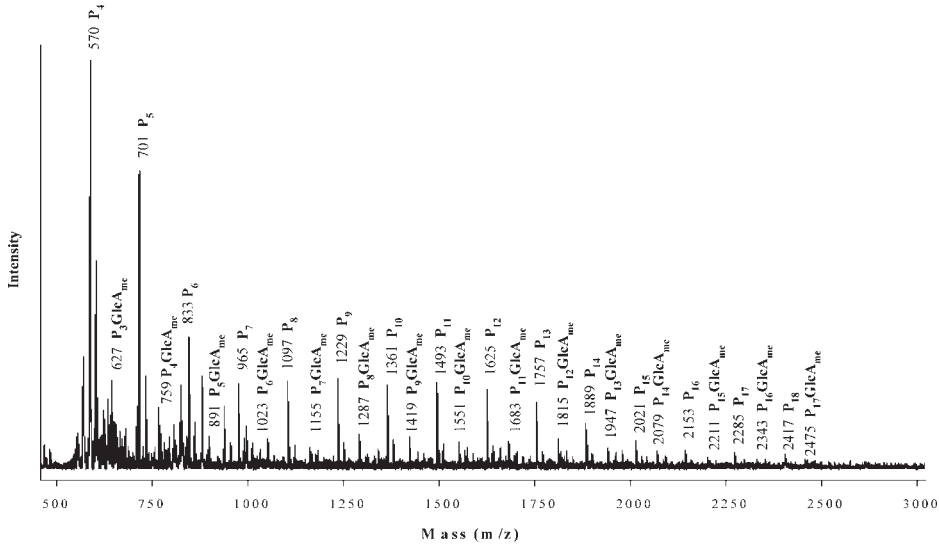

Figure 9.
MALDI-ToF MS spectrum of XOS sample hydrothermolyzed at 120 °C. Masses of the sodium-adducted oligosaccharides are indicated (P = pentose; GlcAme = 4-*O*-methylglucuronic acid).

of acidic XOS with DP from 2 to 16 carrying one 4-*O*-MeGlcA group each were detected. Every oligomer had three isomers. Every one of them could be separately analyzed. Nomenclature described by Domon and Costello was used[35]. The presence of fragment $^{O,2}A_i$ indicates ring cleavage at the reducing end, which confirms that the hydroxyl groups at C-2 and C-3 of the ring are unsubstituted[36]. This leads to the conclusion that the 4-*O*-MeGlcA side chain can not be bound at the reducing end as it could be observed in the spectrum of the first isomer of aldotriouronic acid (MeGlcA-(1,X)-Xyl-(1,4)-Xyl, Figure 10). Further identified fragments were assigned to cleavage of side chain (m/z 289), elimination of water (m/z 461) or formation of B_2- and Y_1-fragments (m/z 329 and m/z 157). C_2- and Z_1-fragments (m/z 347 and m/z 139)[37] were found in very low intensities. The

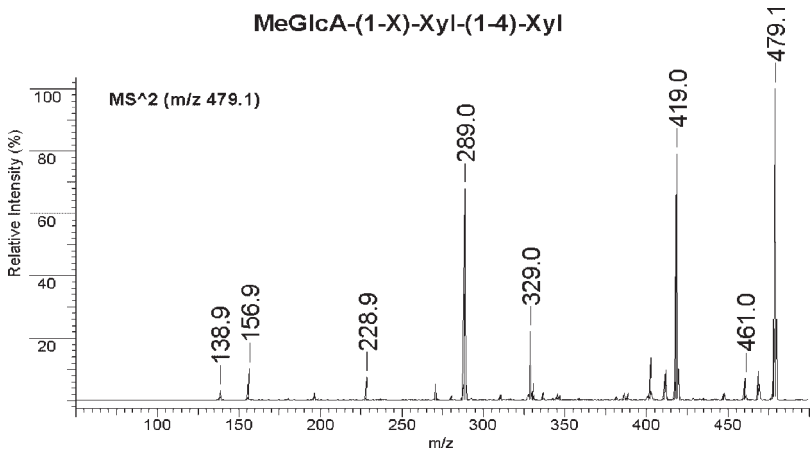

Figure 10.
MS^2-spectrum of aldotriouronic acid, substituted at the terminal end.

© 2006 WILEY-VCH Verlag GmbH & Co. KGaA, Weinheim

Table 6.
m/z-ratios and assigned fragments of aldotriouronic acid isomers.

MeGlcA-(1,X)-Xyl-(1,4)-Xyl		Xyl-(1,4)-[MeGlcA-(1,2)]-Xyl		Xyl-(1,4)-[MeGlcA-(1,3)]-Xyl	
m/z	fragment	m/z	fragment	m/z	fragment
461	B_3	347	$Y_{1\beta}$	461	B_2
419	$^{0,2}A_3$	329	$Z_{1\beta}$	347	$Y_{1\beta}$
329	B_2	289	$Y_{1\alpha}$	329	$Z_{1\beta}$
289	Y_2	257	$^{0,2}X_{0\alpha}$	289	$Y_{1\alpha}$
229	$^{1,3}X_1$	229	$^{0,2}A_{2\beta}$	271	$Z_{1\alpha}$
157	Y_1	197	$B_{1\alpha}$	229	$^{1,3}A_{0\beta}$
139	Z_1	157	$C_{1\beta}$	157	$C_{1\beta}$
		139	$B_{1\beta}$	139	$B_{1\beta}$

C_2-fragment could not be further fragmented due to low intensity. Therefore, it was impossible to determine whether 4-*O*-MeGlcA is bound at C-2 or C-3. Fragments and their corresponding mass/charge-ratios (m/z) are summarized in Table 6.

The spectrum of the second aldotriouronic acid isomer (Figure 11) shows no $^{O,2}A_3$-fragment, indicating that no ring cleavage has occurred and that the 4-*O*-MeGlcA side chain is located at the reducing end. The intensity of the fragment due to elimination of water (m/z 461) is very low, confirming that 4-*O*-MeGlcA is bound at C-2[38]. Elimination of the side chain led to a fragment with m/z 289. Fragments with m/z 139, m/z 347, m/z 157, and m/z 329 could be identified as $B_{1\beta}$-, $Y_{1\beta}$-, $C_{1\beta}$-, and $Z_{1\beta}$-fragments, respectively. In contrast to earlier observations[36], the intensity of the $C_{1\beta}$-fragment was found to be higher than the intensity of the $B_{1\beta}$-fragment.

In the spectrum of the third aldotriouronic acid isomer (Figure 12) again the $^{O,2}A_3$-fragment is missing, supporting the conclusion that the substitution with 4-*O*-MeGlcA is located at the reducing end. The fragment obtained by elimination of water (m/z 461) is of high intensity corroborating that 4-*O*-MeGlcA is bound at C-3 so that the hydroxyl group at C-2 is free for water elimination. This substitution has not been reported in literature yet. Further experiments to confirm this finding are currently under way. The other fragments found were the same as for the *O*-2-substituted isomer, including the higher intensity of the $C_{1\beta}$-fragment if compared to the $B_{1\beta}$-fragment.

Conclusion

Hydrothermolysis was evaluated as a means for XOS production. Xylan isolated from the press-lye from viscose production was converted into a water soluble fraction

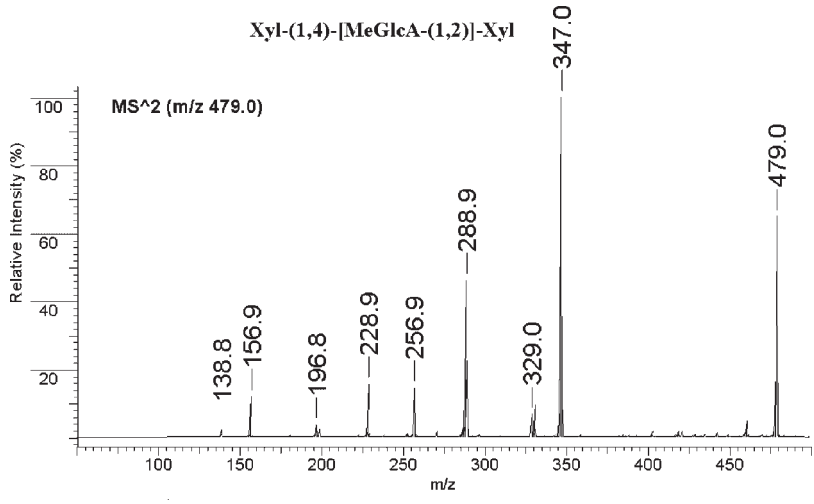

Figure 11.
MS^2-spectrum of aldotriouronic acid, substituted at the reducing end at C2.

© 2006 WILEY-VCH Verlag GmbH & Co. KGaA, Weinheim

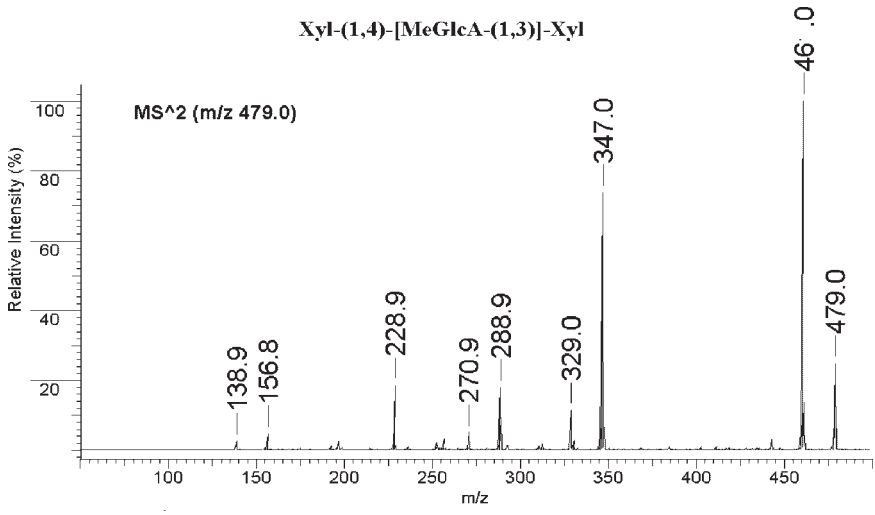

Figure 12.
MS^2-spectrum of aldotriouronic acid, substituted at the reducing end at C3.

and a solid residue. The solid residue was characterized by carbohydrate analysis, SEC, GPC, NMR, and FT-IR measurements. Results corroborated enrichment in glucan along with structural changes in the initial substrate, rendering this residue unsoluble. A mass balance was established to determine weight loss kinetics. On this basis the activation energy for xylan hydrothermolysis could be calculated, resulting in a value of 169.7 kJ/mol. The soluble fraction contained neutral and acidic XOS. Neutral XOS were separated and quantified using HPAEC-PAD. The DP distribution of the XOS could be varied in a wide range by the reaction parameters time and temperature. Acidic XOS were analysed by MS^2 to identify the exact positions of the 4-*O*-MeGlcA side chains. Three different isomers could be detected and identified. A low amount of 4-*O*-methylglucuronic acid bound to *O*-3 of the xylan backbone could be accounted for in the acidic XOS mixture, which has not been reported in literature yet.

Acknowledgements: Financial support was provided by the Austrian government, the provinces of Lower Austria, Upper Austria and Carinthia as well as by the Lenzing AG. We also express our gratitude to the Johannes Kepler University, Linz, the University of Natural Resources and Applied Life Sciences, Vienna, and the Lenzing AG for their in kind contributions. MALDI-measurements were carried out in Wageningen, The Netherlands, by Prof. Henk A. Schols. Metal components were determined by Prof. Richard Tessadri in Innsbruck, Austria. We give special thanks to our collegue Dr. Fasching for his expressive help.

[1] R. Vegas, J.L. Alonso, H. Domínguez, J.C. Parajó, *Ind. Eng. Chem. Res.* **2005**, *44*, 614.
[2] E. Walch, A. Zemann, F. Schinner, G. Bonn, O. Bobleter, *Bioresource Technology* **1992**, *39*, 173.
[3] D. Fengel, G. Wegener, in: "*Wood: Chemistry, Ultrastructure, Reactions*", de Gruiter, 1984.
[4] B. Lindberg, K. G. Rosell, S. Svensson, *Svensk Papperstidning* **1973**, *1*, 30.
[5] P. Hoffmann, R. Patt, *Holzforschung* **1976**, *30*, 124.
[6] T. Iversen, B.O. Lindgren, *Das Papier* **1983**, *37*, 573.
[7] H. Sixta, N. Schelosky, W. Milacher, T. Baldinger, Th. Röder, *Proceedings of the 11th ISWPC* **2001**, *Vol. 3*, 655.
[8] J. Puls, Th. Kruse, B. Saake, 10th ISWPC, Yokohama, **1999**, June 7–10, 54.
[9] K. Ishii, R.D. Teasdale, *Plant Cell, Tissue and Organ Culture* **1997**, *49*, 189.
[10] Fooks, Fuller, Gibson, *International Dairy Journal* **1994**, *9*, 53.
[11] H.W. Modler, *International Dairy Journal* **1994**, 383.
[12] Q. P. Yuan, H. Zhang, Z. M. Qian, X. J. Yang, *J. Chem. Technol. Biotechnol.* **2004**, *79*, 1073.
[13] O. Dahlman, A. Jacobs, A. Liljenberg, A. I. Olsson, *Journal of Chromatography A* **2000**, *891*, 157.
[14] J.C. Parajó, G. Garrote, J.M. Cruz, H. Domínguez, *Trends in Food Science and Technology* **2004**, *15*, 115.

© 2006 WILEY-VCH Verlag GmbH & Co. KGaA, Weinheim

[15] M. J. Vázquez, J. L. Alonso, H. Domínguez, J. C. Parajó, *Trends in Food Science and Technology* **2001**, *11*, 387.
[16] G. Garrote, H. Domínguez, J. C. Parajó, *J. Chem. Technol. Biotechnol.* **1999**, *74*, 1101.
[17] G. Garrote, J.C. Parajó, *Wood Sci. Technol.* **2002**, *36*, 111.
[18] G. Garrote, H. Domínguez, J. C. Parajó, *Ind. Eng. Chem. Res.* **2004**, *43*, 1608.
[19] M. A. Kabel, F. Carvalheiro, G. Garrote, E. Avgerinos, E. Koukios, J. C. Parajó, F. M. Girió, H. A. Schols, A. G. J. Voragen, *Carbohydrate Polymers* **2002**, *50*, 47.
[20] A. Teleman, T. Hausalo, M. Tenkanen, T. Vuorinen, *Carbohydrate Research* **1996**, *280*, 197.
[21] R. Vegas, J. L. Alonso, H. Domínguez, J. C. Parajó, *J. Agric. Food Chem.* **2004**, *52*, 7311.
[22] B. Philipp, W. Rehder, H. Lang, *Das Papier* **1965**, *19*, 1.
[23] Blumenkrantz, Asboe-Hansen, *Anal. Biochem.* **1973**, *54*, 484.
[24] U. Mais, H. Sixta, in: "*ACS-book – Xylans, Mannans and other Hemicelluloses*", **2002**.
[25] A. Jacobs, P.T. Larsson, O. Dahlman, *Biomacromolecules* **2001**, *2*, 979.
[26] M. A. Kabel, H. A. Schols, A. G. J. Voragen, *Carbohydrate Polymers* **2001**, *44*, 161.
[27] S. Veerarathavan et al., AIChE National Meeting, **1982**, Orlando, FL
[28] A.H. Conner, *Wood and Fiber Science* **1984**, *16*, 268.
[29] H. Sixta, Habilitation, 1995, Technical University Graz, Austria
[30] O. Bobleter, in: "*Polysaccharides*" 2nd ed., 2005, 893.
[31] D. F. Root, J. F. Saeman, J. F. Harris, W. K. Neill, *Forest Prod. J.* **1959**, *9*, 158.
[32] K. Schoenemann, *Chem. Eng. Sci.* **1957**, *8*, 161.
[33] A. Gandini, *Adv. Polym. Sci.* **1977**, *25*, 47.
[34] D.L. VanderHart, R.H. Atalla, *Macromolecules*, **1984**, *17*, 1465.
[35] B. Domon, C. Costello, *Glycoconjugate J.* **1988**, *5*, 397.
[36] G.E. Hofmeister, Z. Zhou, J.A. Leary, *J. Am. Chem. Soc.*, **1991**, *113*, 5964.
[37] B. Spengler, J.W. Dolce, R. Cotter, *J. Anal. Chem.* **1990**, *62*, 1731.
[38] A. Teleman, M. Tenkanen, A. Jacobs, O. Dahlman, *Carbohydr. Res.* **2002**, *337*, 373.

© 2006 WILEY-VCH Verlag GmbH & Co. KGaA, Weinheim